7 Examples of Exact-Constraint Designs

This chapter presents particular exact-constraint designs that are being used for the NIF and EUVL projects. These designs use both flexural elements and contacting surfaces as constraint devices. All the designs have been thoroughly analyzed using various techniques, but this chapter is about design rather than analysis. The intent is to present the thinking behind the designs. Where it is of interest, analytical or experimental results will be mentioned. Most of the figures in this chapter are photographs of hardware. All efforts have been made to ensure good quality, but photographs sometimes do not reproduce well.

7.1 Optic Mounts for EUVL Projection Optics

The key requirements for EUVL projection-optic mounts are as follows:

- Provide rigid and stable location of the optic with respect to the main structural component, called the projection optics box.
- Apply negligible forces and moments to the optic other than those required to support the weight of the optic.
- Provide a repeatable connect-disconnect capability so that the optic can be processed separately from the mount and returned to a repeatable location and state of strain.

Each projection optic in the system has an additional requirement that is satisfied at a higher system level by a unique design, but all those designs incorporate the same basic mount design described here. Later sections describe those higher-level requirements and design solutions. These requirements common to all the optics are satisfied by a structural element called an optic cell and an ideally kinematic coupling between it and the optic.

The desire for symmetry and the minimum number of physical connections to the optic led to a general configuration using three pairs of constraints. The sphere-vee constraint is conceptually simple but high stiffness in the unconstrained directions (i.e., before sliding occurs) is a concern due to differences in thermal expansion between the optic and the cell. Another concern is the contact stress that would result on the low-thermal-expansion materials being considered such as super invar and Zerodur™. The configuration that appears in Figure 6-6 (a), three sets of sphere-cone constraints each with a radial-motion flexure, solves the contact stress problem, but the sphere-cone constraint is still stiff in rotational degrees of freedom. For example, a portion of the loads applied to the cell transfers through the optic mount and into the optic. This problem is greatly reduced by adding three more flexural degrees of freedom. The result is the bipod flexure, a two-constraint device. A set of three bipods can provide nearly ideal kinematic support for super-precision optics and other sensitive instruments. Figure 7-1 shows a typical mount design with and without the optic installed.

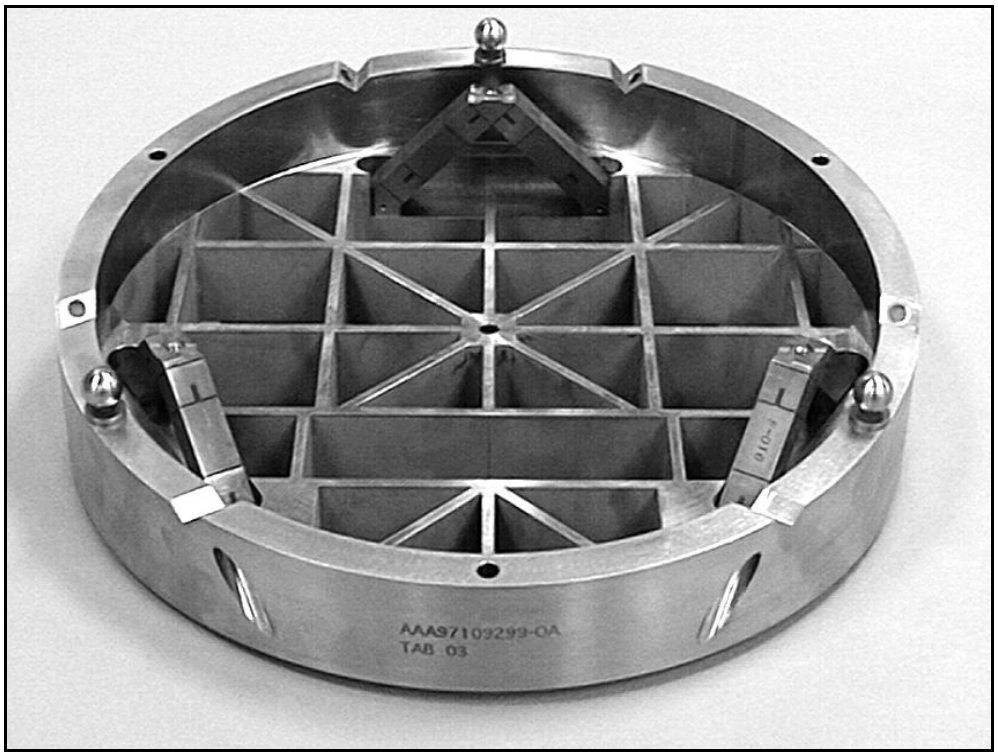

(a)

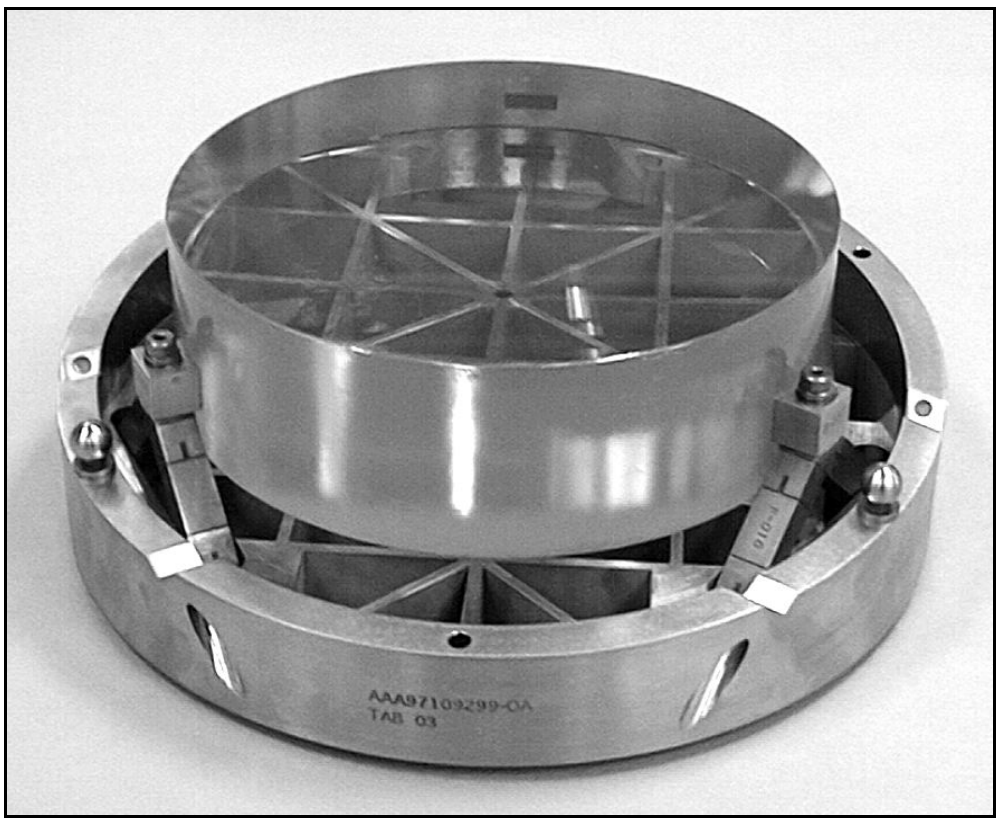

(b)

Figure 7-1 The optic cell and three bipod flexures (a) present three small kinematic couplings that engage three lugs bonded to the optic (b). A coil spring held with a shoulder screw provides the preload for each coupling. The lugs are boned to the optic while attached to relaxed bipod flexures, and subsequently the assembly becomes matched for life. The individual three-tooth couplings are repeatable to the micron level.

While the decision to use three bipod flexures was fairly obvious and unconstrained, the opposite was true for the type of connection to make between each bipod and the optic. One design constraint was the need to order the optic substrate material before there was time to design the mounts. This and the desire to keep the optics as simple as possible led to the decision to epoxy bond mounting features to the semifinished optic that would arrive months later. The other primary decision was the type of connect-disconnect device to use at each bipod. The sphere-cone constraint is simple and effective, but it comes with the risk that significant *noise* moments can exist in the bipods depending how the optic is installed in the mount. A significant noise moment for these optics is a few newton-millimeters. Ultimately we chose to use the three-tooth coupling, a fully constraining connection. The positional repeatability of the coupling ensures very good elastic repeatability of the flexures. Further, the technique used to bond lugs to the optic puts the bipod flexures very nearly in a relaxed stress state.

The decisions made for this projection optics system, being a fast-track experimental tool, are not necessarily appropriate for future production tools. For example, an issue with the epoxy bond is long-term dimensional stability. Measurements of loaded samples extrapolated in time indicate that the system may drift out of optical alignment in perhaps 6 to 12 months (thus requiring an off-line realignment of optics).[I] This is obviously not acceptable for a production tool and the positional requirements probably will become more stringent in the future. It becomes apparent that future designs will require direct connections between the optic and the mount. An epoxy bond could be used as a fastener, for example, in conjunction with a compliant element to apply a preload, but the interface that determines stability should not be a polymer.

Given this insight, the sphere-cone constraint becomes a favorite because three cones are easily manufactured directly into the optic. The cell would present three small spheres mounted on bipod flexures, for example. There are techniques available to make the optic less sensitive to noise moments at the constraints, and the installation process can be made more deterministic to reduce noise moments. In addition, there is no particular limitation with this design from being able to process the optic in one cell and use it in another. This would be very difficult to do with fully constraining couplings. Other aspects may also come into play such as combining actuated alignment mechanisms within the optic mount. Presently the cells are manipulated by alignment mechanisms, but it is difficult to achieve the very high resonance frequencies desired for such systems with a series arrangement of constraints.

[I] Experiments were performed at the University of North Carolina Charlotte [Patterson, et al., 1998] and LLNL.

7.2 A Gravity-Compensating Optic Mount for EUVL

Three of the projection optics are manufactured using vertical-axis fabrication metrology to match the orientation of the projection optics system. These optics will have the proper figure when mounted rather than in the free state, assuming of course that the mount is absolutely repeatable. One optic in the system is an exception because its large radius of curvature makes a vertical-axis interferometer impractical. With the optic supported in a sling, horizontal fabrication metrology produces an optic with the proper figure nearer the free state, especially when using multi-step averaging. It then becomes necessary to compensate for the different mount and the change in gravity orientation.

A finite element model of the optic supported at three perimeter points, as with three bipods, revealed unacceptable gravity-induced figure error. Figure 7-2 (a) shows the figure error within the clear aperture after removing the best-fit sphere.[I] The dominant error is trifoil produced from the three supports. By distributing the weight over nine perimeter points, the error becomes primarily spherical, which the system will tolerate with a focus adjustment. The remaining nonspherical error in (b) is more than an order of magnitude less than in (a). For comparison, the P-V error goes from 1.62 nm to 0.107 nm and the rms error goes from 0.314 nm to 0.027 nm.

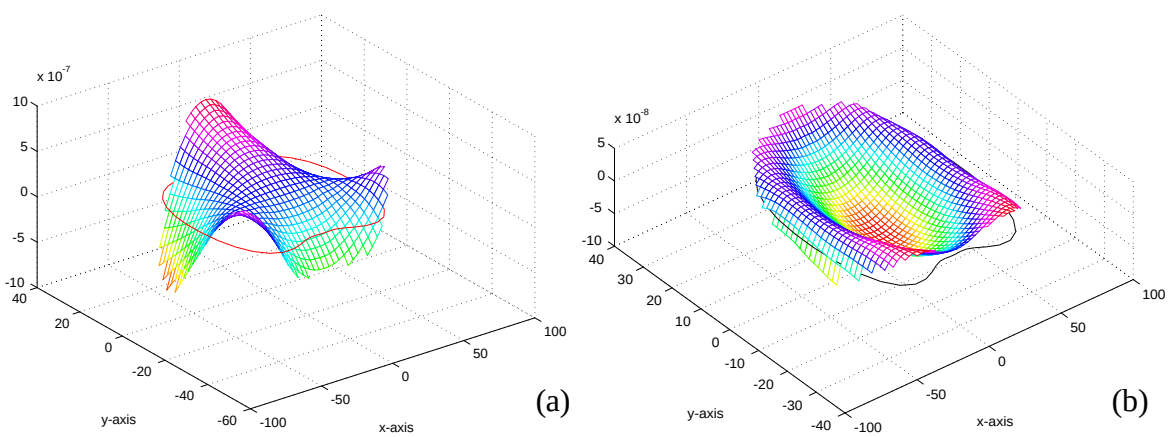

Figure 7-2 Figure error (in mm) over the clear aperture with three supports (a) and nine supports (b).

The gravity-compensating optic mount supports the weight of the optic at nine locations around the perimeter. Three of the nine supports are rigid bipod constraints as used in the other three optic mounts. The remaining six supports are compliant springs that provide weight relief but no constraint. The tension is set according to modeling results that minimize the nonspherical error over the clear aperture. Figure 7-3 shows the design for the projection optics system in (a) and a demonstration test optic and mount in (b).

[I] Pro/MECHANICA™ by Parametric Technology Corp. is the finite element software used in this study. MATLAB™ by The MathWorks, Inc. is the computing environment used to process the finite-element results and create the surface plots.

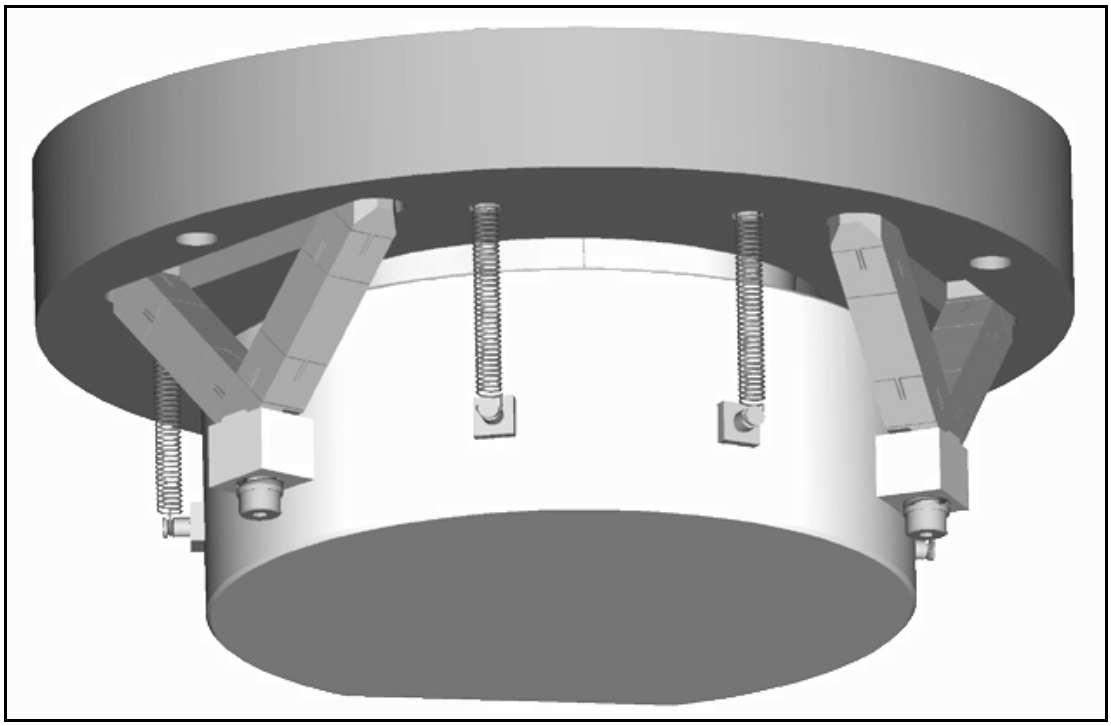

(a)

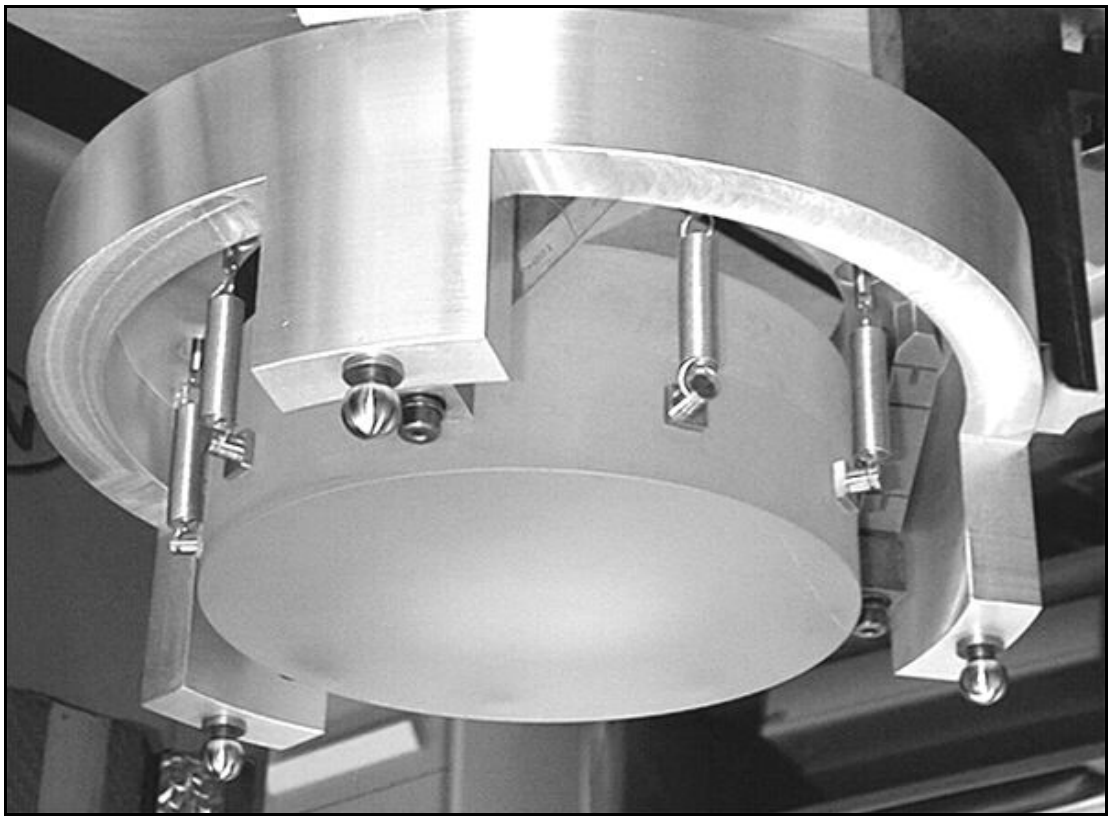

(b)

Figure 7-3 The gravity-compensating optic mount supports the weight of the optic at nine locations around the perimeter using three rigid bipod constraints and six compliant springs. The model in (a) is the design for the projection optics system. A demonstration test optic and mount appear in (b).

7.3 θ_x-θ_y-Z Flexure Stage for EUVL Projection Optics[I]

Two of the projection optics require remotely actuated alignment degrees of freedom in θ_x, θ_y and z, where z is the optical axis. This out-of-plane motion may be accomplished by translating any three perimeter points appropriately in the z direction. Effectively, these three translations are adjustable constraints. Three more passive constraints provide exact constraint for the suspended object, in this case for the optic cell. Although a 3-2-1 constraint arrangement is possible, the natural choice is three identical pairs of constraints, where one direction is actuated and the other is passive. This is the arrangement shown in Figure 7-4 for a prototypical optic, cell and actuation system.

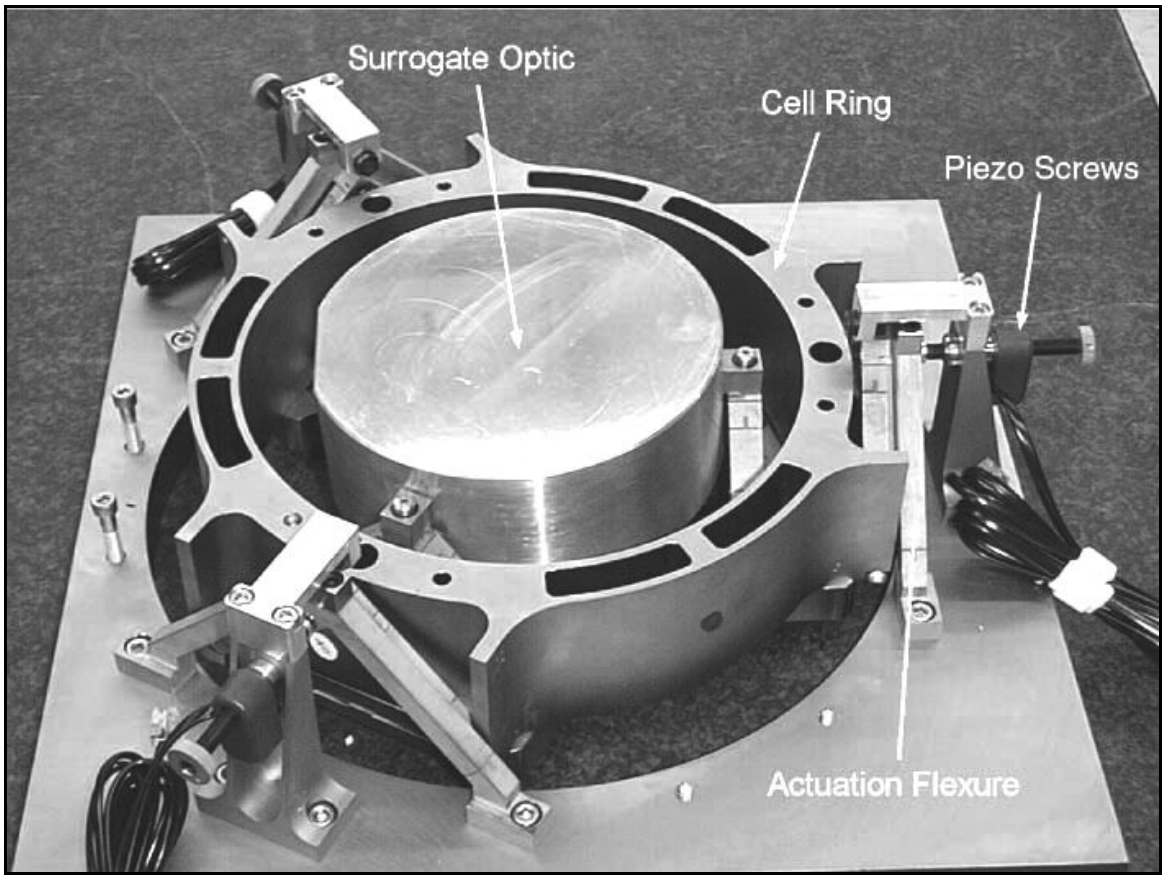

Figure 7-4 Three sets of actuation flexures support the optic cell relative to a base plate. Each actuation flexure transfers radial motion from a piezo-driven screw to axial (z) motion of the cell through a 5:1 reduction ratio. The cell then supports the optic passively through three bipod flexures.

The actuation system consists of three actuation flexures that support the optic cell relative to the projection optics box and a set of three piezo-driven screws that actuate the flexures. The actuation flexure provides both passive constraint tangent to the cell and a 5:1 transmission ratio between the screw and z motion at the cell. The screw provides the

[I] This material was previously published in greater detail [Tajbakhsh, et al., 1998].

actuated constraint through the 5:1 reduction ratio, thereby providing better resolution to the cell. Figure 7-5 shows more clearly the functional parts of the actuation system and the flexure cuts that provide the necessary freedoms.

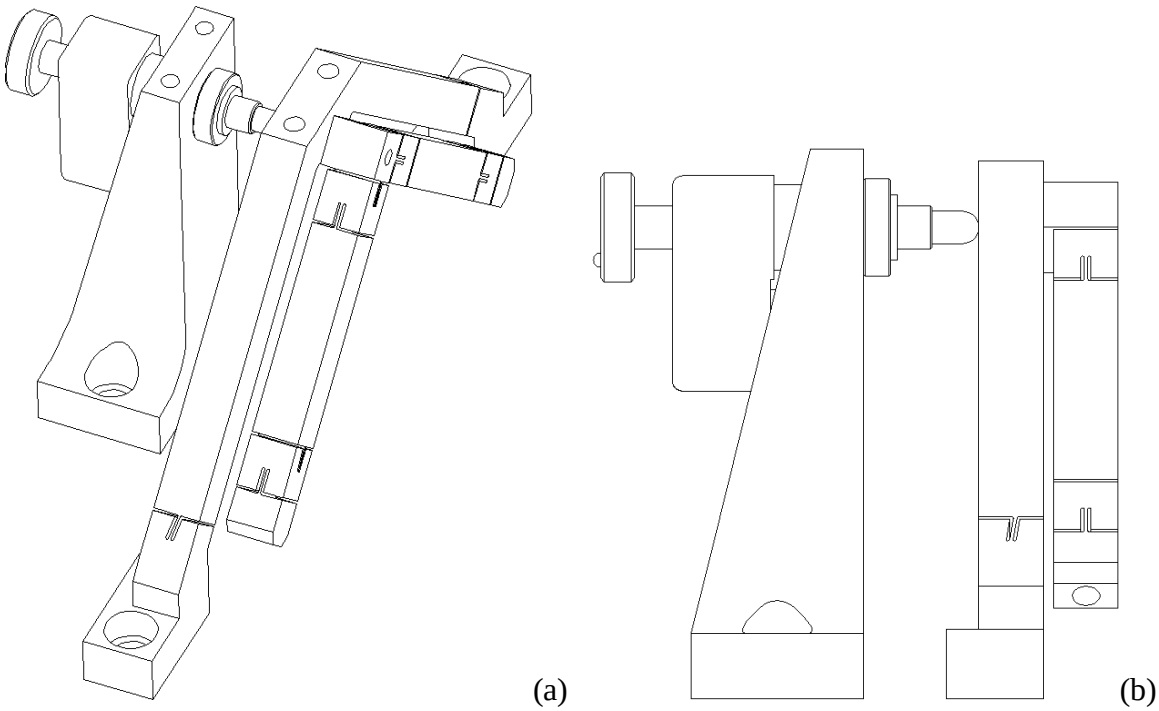

Figure 7-5 The actuation flexure consists of a supporting hinge flexure connected to a bipod. In (b), the 5:1 lever ratio is more apparent between horizontal motion of the screw and vertical motion of the cell.

The actuation flexure is physically one piece of super invar that has been cut out as shown using wire EDM (electro-discharge machining). Functionally, it consists of the constraint side that attaches to the cell and a transmission side that connects to the base structure. The constraint flexure is the same basic bipod design that is used for optic mounts. It provides local angular freedom to the cell while transferring two constraints from the transmission flexure. The instant center (where the two constraints intersect) is placed in the plane of the optic so that the rotation axis will also be in this plane. The transmission flexure is a simple hinge axis that is controlled by the screw position. A subtle aspect is the angle of the blade whose plane intersects the instant center of the constraint flexure. Effectively the forces in the bipod flexure transfer to the transmission flexure through this point. If the screw also acts through this point, then there is no out-of-plane force on the blades. The angle of the plane defined by the hinge axis and the instant center determines the transmission ratio between the screw and the cell.

There are two main design issues with this actuation flexure. The first is the moment imparted to the cell during actuation. This could be alleviated by placing the hinge point adjacent to the instant center, but this would require a cross flexure rather than a simple hinge. The finite element model shows no problems with this design because the cell is

sufficiently stiff. It would become a problem if the cell were eliminated in a future design with the optic directly supported on actuation flexures. The second issue is bending compliance in the transmission side since much of its structure lies outside the plane between the hinge axis and the instant center. This is the main compliance in the prototype system whose first constrained mode is 133 Hz. In an effort to push towards 200 Hz, the transmission side is now substantially thicker and joined across the legs.

It is interesting to state some of the experimental results of the prototype system. As mentioned the first constrained mode is 133 Hz, but it is remarkable and perhaps coincidental that FEA and experimental modal analysis gave the same number. Actually there are two modes at this frequency corresponding to any two orthogonal translations in the *x*-*y* plane. The remaining modal frequencies are 200 Hz and above. The dynamics of the optic with respect to the cell is rather insignificant. The positioning resolution demonstrated by this system is 2 to 3 nanometers as determined by capacitance gauge feedback. The screws are controlled in a low-bandwidth loop until the final position is reached, then they are turned off. All the main structural components are super invar except for the commercially available piezo-driven screws.

7.4 X-Y Flexure Stage for EUVL Projection Optics

One projection optic requires remotely actuated alignment degrees of freedom in *x* and *y*, where *z* is the optical axis. This optic is spherical and physically smaller than the other three aspheric optics. Being spherical, it then is acceptable for the optic to rotate as it translates. This allows the possibility of a rotational axis being used to translate the optic. Being smaller, it becomes practical to build the alignment mechanism directly into the optic cell. The X-Y-θ_z stage that uses three folded-hinge flexures is a natural starting point for this design (see Chapter 6.1.3). It merely requires one less actuated degree of freedom.

Figure 7-6 shows the design for the optic cell and integrated alignment mechanism. As with the other optics, three small bipod flexures support the optic relative to the cell. The cell has three areas that attach directly to the projection optics box as indicated by mounting holes. The rest of the cell articulates on the flexures. For motion in the *x*-*y* plane, each folded-hinge flexure provides one actuated constraint along the constraint side of the flexure (using the same terminology as the previous section). The single flexure at the top provides one passive constraint in the *x*-*y* plane. The constraint lines for these flexures (indicated by centerlines) form the instant centers about which the optic rotates. Extending actuator 1, for example, moves the optic down and to the right. If both actuators extend equally, then the optic translates downward without rotation. If both actuators extend equal amounts in opposite directions, then the optic rotates about the center of the passive constraint. The 30˚ angle between the transmission and constraint flexures provides a 2:1 reduction ratio between the actuator and the constraint line. There is another reduction ratio of approximately 1.4:1 resulting from rotation about either instant center.

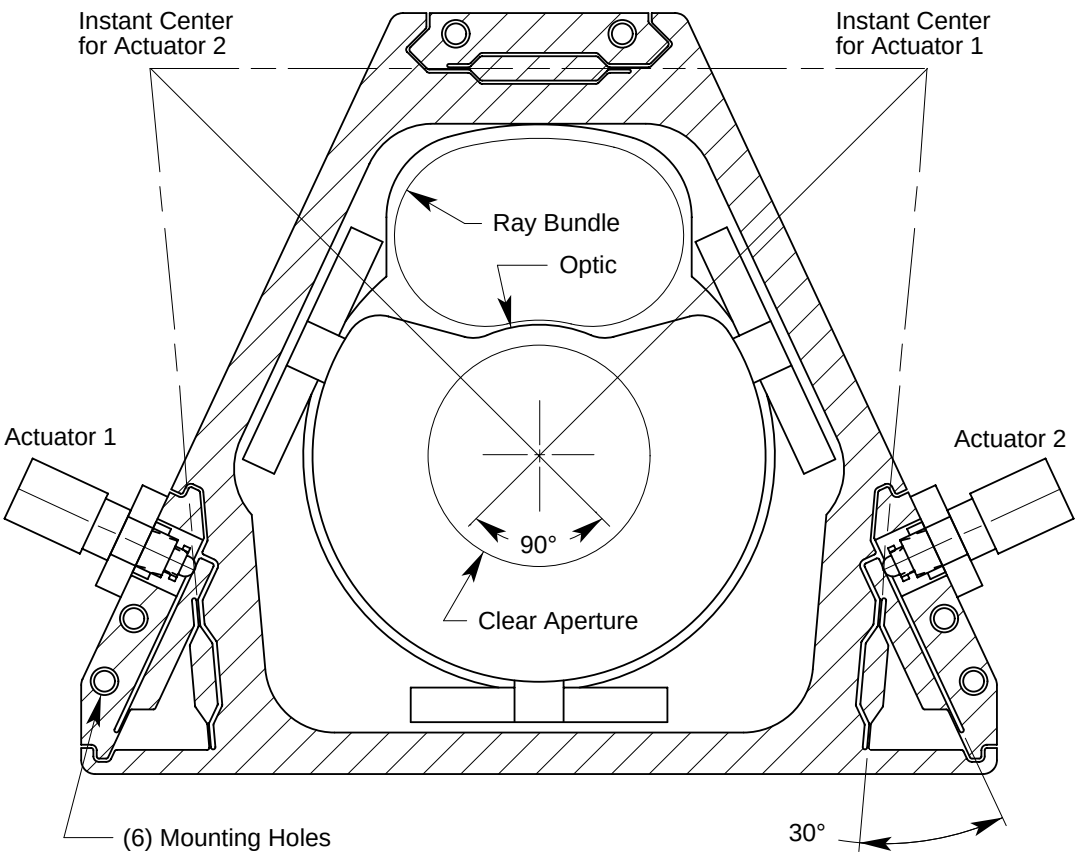

(a)

(b)

Figure 7-6 In (a), a cross section through the optic cell shows the details of the flexures and the instant centers about which the optic rotates. In (b), the optic cell interfaces to the interferometer through a three-vee coupling. The black ears with tooling balls are removed from the cell after interferometry is complete.

The three out-of-plane degrees of freedom are overconstrained in this design by one extra constraint. Each folded-hinge flexure provides one z constraint while the single flexure provides two constraints, z and θ_y. The consequences of overconstraint will be some residual stress in the cell, flexures and the supporting structure. Although the surfaces that bolt together are precisely machined, they may require some hand fitting at assembly. This overconstraint will not affect the freedom of motion in the *x-y* plane.

The modal frequencies as predicted by FEA are quite high for this design. The first mode at 289 Hz results primarily from the flexibility of the folded-hinge flexures in their passive constraint direction. The next two modes are in the general direction of the actuated motions. Rotation about the passive constraint occurs at 354 Hz and translation (up and down) occurs at 436 Hz.

7.5 Kinematic Mounts for NIF Optics Assemblies

The basic kinematics and the optimization analysis for this example are treated in Chapter 6. This section presents the design solution and explains the main decisions made through the design process. The key requirements for the NIF kinematic mounts are as follows:

- Provide stiff, repeatable location in six degrees of freedom.
- Allow straight-line installation of the assembly from underneath.
- Provide the maximum amount of clearance and capture range within the space constraints of the closely packed laser beams.
- Provide secondary safety support and seismic restraint.
- Operate in accordance with class 100 clean room requirements.

The last two requirements are not discussed other than to say that a separate mechanism provides seismic restraint, effectively holding the kinematic mounts together, and that all the parts are corrosion resistant and easy to clean. Since the operation is infrequent and the mechanisms operate under essentially no load, particle generation is not expected to be problem. The first three requirements govern the kinematic mount design described here.

The architecture for the NIF laser system is heavily influenced by the need to routinely replace damaged optics in a very clean and inert atmosphere. A concept was developed where any optics assembly, known as a line replaceable unit or LRU, could be installed or removed from underneath the beam line of the laser.[I] The LRU being installed is transported in a clean canister from the clean assembly area to the beam line. The canister docks to the laser structure using a kinematic coupling, establishes a pressure-tight seal,

[I] As the design matured, some types of LRU's were easier to load from the top or the side, but most still load from below.

removes an access panel, and installs the LRU with a straight-line lift.[I] The interface between the LRU and the canister lift platform is also kinematic and preloaded by gravity.[II] Yet another kinematic coupling supports the LRU from the laser structure. This is the kinematic mount that must satisfy the requirements stated above. A prototype LRU for periscope optics appears in Figure 7-7 along with close-up views of the kinematic mounts.

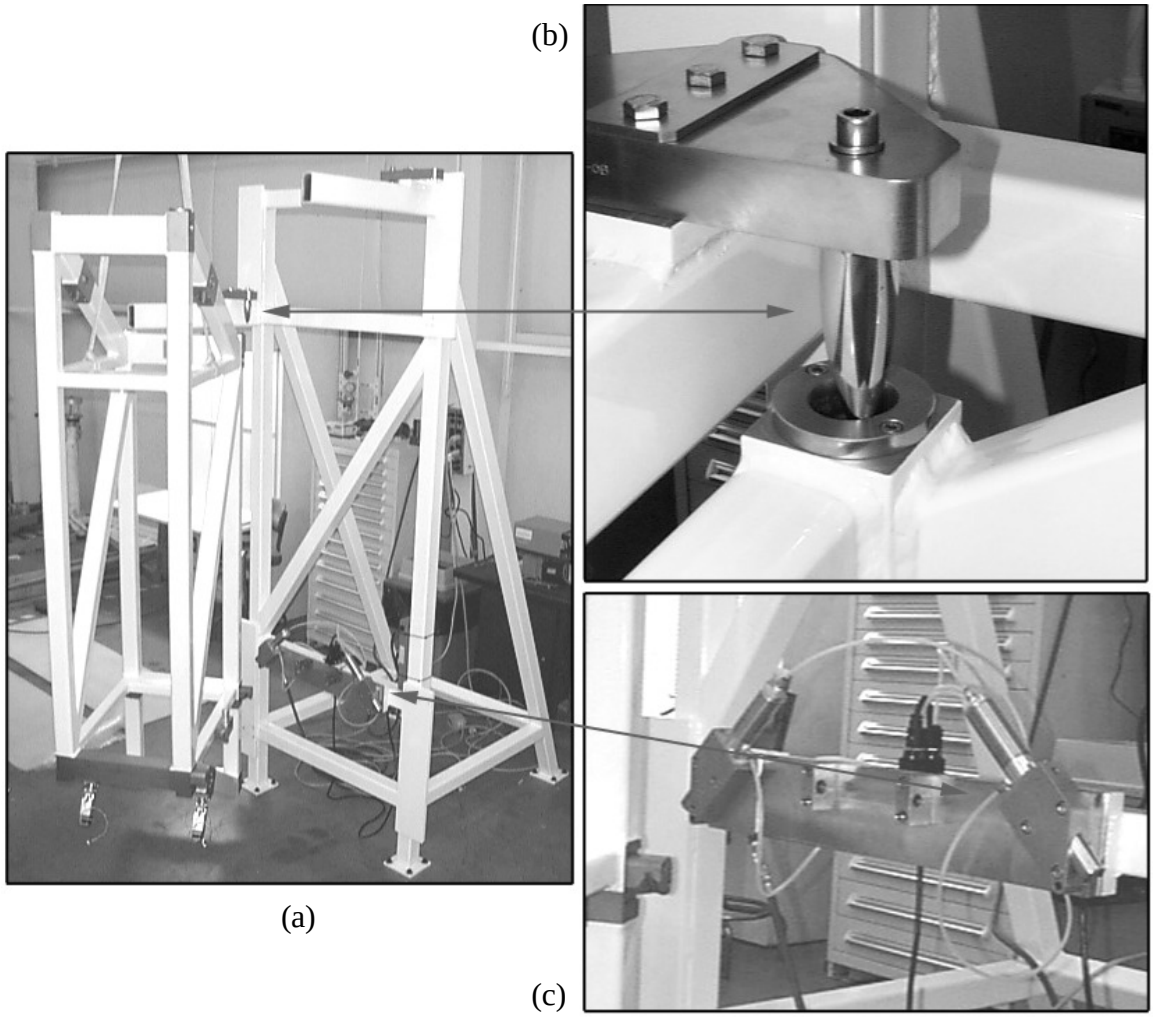

Figure 7-7 The prototype LRU in (a) is temporarily supported by a crane to better show the kinematic mounts. The LRU is over 2.5 m tall, and when mounted in the NIF periscope structure, the lowest point will be 3.6 m to 5.5 m above the floor. The upper mount has two pin-slot constraints like the one shown in (b) partially engaged. The pin attaches to the structure and is Ø 35 mm. In (c), two vee blocks on the LRU engage two Ø 32 mm actuated pins on the structure to form the lower mount.

[I] The kinematic coupling consists of three conical seats in the bottom of the laser structure and three spheres attached to the top of the canister each with a hinge axis to release the radial constraints. The upward preload is provided by the transporter that carries the canister.

[II] The bottom of the LRU has conical sockets that engage spheres on the canister lift platform each having the appropriate flexural freedom.

The upright shape and dense packing of LRU's combined with demanding stability requirements (0.6 μr rms at the optics from all sources) constrained the mounting points to lie in a vertical plane to give the most favorable aspect ratio. Further, FEA showed that the torsional mode of the LRU frame would be a limitation to achieving the vibrational part of the stability budget. This assumes that the one end is torsionally constrained, say with two vees, and the other end is free to rotate about the third vee.[I] The modal frequency can be increased somewhat by placing the instant center of the vee near the principal axis, thereby reducing the mode's moment of inertia. This naturally leads to a widely spaced vee, which has the more significant benefit of adding a stiff, frictional constraint against rotation. For example, the stiffness of this frictional constraint is an order of magnitude stiffer than the LRU frame. On the other hand, tangential friction forces in the constraints could potentially twist the frame up to 40 μr from the free state, but this is much less than the requirement for initial alignment. It is only important that the twist remains constant.

One very basic choice made early in the design process was to use gravity to preload the kinematic mount. Frankly, the alternative (a latching mechanism that would preload the LRU up against a passive kinematic coupling) was not explored as thoroughly as it should have been. Either case requires a mechanism that allows a straight-line insertion from underneath and then restrains both gravity and potential seismic loads. In the beginning, probably not enough consideration was given to the seismic load. A mechanism that works in concert with gravity would seem to be simpler than one that must defeat gravity. It is easy to become convinced this way when you have a workable concept in mind and have not carefully thought through the alternatives. Another aspect that seems to favor a gravity-loaded kinematic mount is the freer transfer of the LRU from the canister lift platform, also a gravity-loaded kinematic coupling. The weight transfers in a smooth hand off from one coupling to another as the platform rises or lowers.

The basic configuration of the LRU kinematic mount is a three-vee coupling with one widely spaced vee at the top and two vees near the bottom. The upper vee is passive with two pin-slot constraints that engage as the LRU lifts into place. The lower mount is active and formed by two vee blocks on the LRU that can pass by retracted pins on the structure. The pins extend to receive the vee blocks and support the weight of the LRU. The details of these will be presented later. This design is an inversion of the original concept that had two actuated pins mounted near the top of the LRU. There were differing opinions as to the better arrangement. The final decision was made by a fairly diverse group of twelve people using the Analytic Hierarchy Process. The results through the first criteria level appear in Table 7-1. Some of the key factors in this decision were: 1) the preference to place potential particle generators below optics, 2) better personnel access in case the mechanism failed to

---

[I] Had there been space around the LRU, a reasonable approach would be to place three vees in a horizontal plane at the middle elevation. It still may have been difficult to meet the stability budget.

release, 3) avoid remotely breaking pneumatic lines between the LRU and the canister, and 4) better capture range provided by a passive upper mount.

AHP Design Spreadsheet				
Created by L. Hale 2/27/97				
	Decision:	10	10	10
Criteria Level 1 >	1.00	Functionality	Design Issues	Maintenance
Criteria Level 2 >		0.33	0.33	0.33
Design Options				
Active mount location				
> LRU - upper	5.23	3.62	6.26	6.32
> LRU - lower	6.77	3.91	7.94	10.00
> Structure - upper	5.01	3.83	7.88	4.16
> Structure - lower	7.42	5.54	10.00	7.37

Table 7-1 The AHP helps provide a global picture of the decision while focusing attention to specific details. The design options were evaluated at Criteria Level 2. These are: Loading, Centering and Cleanliness under Functionality; Clearances, Seismic and Pneumatics under Design Issues; and Reliability, Release Access and Repair Access under Maintenance.

The pin-slot constraints of the upper mount provide a simple, passive engagement upon inserting the LRU into position. As Figure 7-8 shows, each constraint consists of a tapered pin attached to the structure and a slotted receiver at the top of the LRU. The combination provides the top of the LRU with approximately 15 mm of radial capture range. The upward-facing receiver also tends to catch any wear particles generated from the siding surfaces. The vee angle formed by the slots was determined to optimize centering ability as discussed in Chapter 6. This angle varies among different types of LRU's but the worse-case load governs the design of these parts that are in common. Managing the contact stress is the primary design problem for relatively heavy loads, and the need for capture range makes it difficult to use closely conforming surfaces. After working through the compromises, the results of the contact analysis appear in Table 7-2. The materials are the same as used on the lower mount and will be discussed later.

Analysis for Upper Mount		
Pin's principal radii of curvature	R_{xx} = 215 mm	R_{yy} = 17.5 mm
Slot's principal radii of curvature	R_{xx} = 45 mm	R_{yy} = inf. (straight)
Load cases: nominal and 4x nominal	P = 90 kgf	P = 4 (90) kgf
Contact pressure (compressive stress)	p = 223 ksi	p = 353 ksi
Maximum shear stress (no sliding)	τ = 72.5 ksi	τ = 115 ksi
Equivalent tensile stress $\sigma = \sqrt{3}\,\tau$	σ = 125 ksi	σ = 199 ksi
Approach of distant points	δ = 11 μm	δ = 27 μm
Stiffness at the nominal load	k = 0.70 Mlb/in	

Table 7-2 Two load cases are provided for the upper mount at full engagement. Four times the nominal load represents a dynamic overload that might occur in an earthquake. A nominal load at initial engagement has nearly identical stress as the overload case.

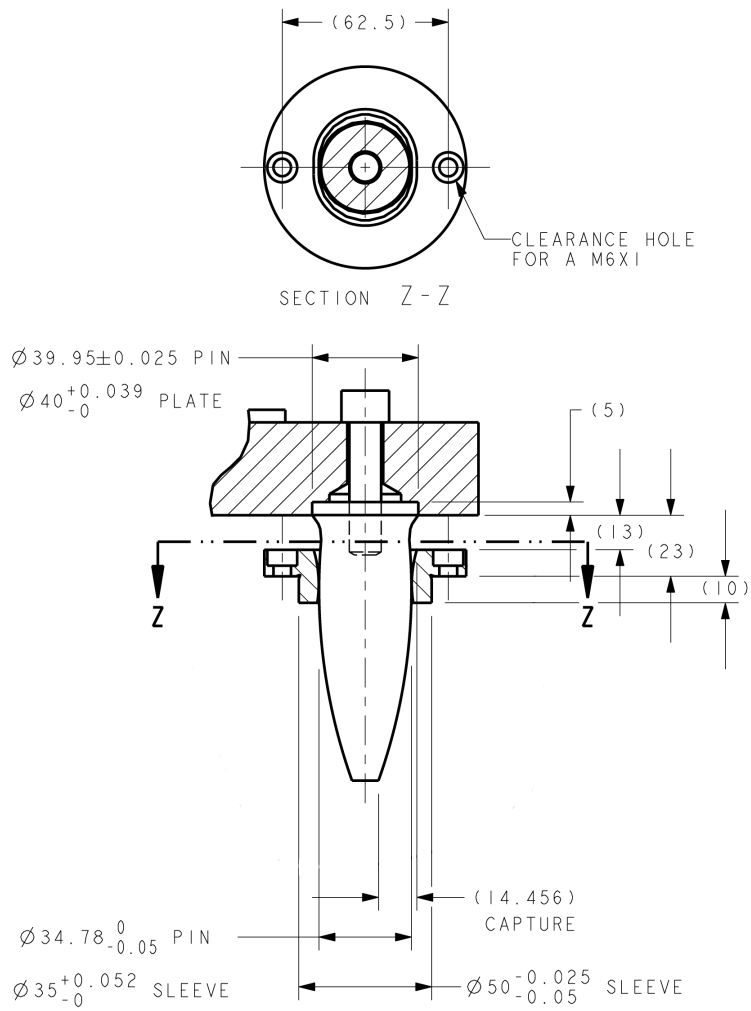

Figure 7-8 The slotted receiver at the top of the LRU engages the tapered pin attached to the structure.

The lower active mount consists of right- and left-hand assemblies of identical parts. For example, Figure 7-9 shows the left-hand assembly. Each vee block bolts to the LRU with the contact surfaces pointing down and towards the center. These surfaces are revolved so that contact with the pin occurs at two local areas. Each pin mechanism bolts to the structure and is actuated by a pneumatic cylinder. For safety reasons, the 1.50 inch bore cylinder operating at 60 psig is incapable of retracting under the weight of the lightest LRU. For control purposes, a pair of photodetectors in the canister sense retroreflective tape on the vee blocks. When the pins have extended far enough to block the return beams, it then is safe for the LRU to be lowered onto the pins. This avoids placing many hundreds of limit switches within the beam line. The angles of the pins and the surfaces of the vees were determined to optimize centering ability as discussed in Chapter 6. Due to the angle of the pin, the load is primarily compressive across its 32 mm diameter. In other words, the pin bridges the gap between the vee block on the LRU and the bore of the housing that guides the pin. The pin diameter, capture ranges and clearances between parts are as large as possible given the available space.

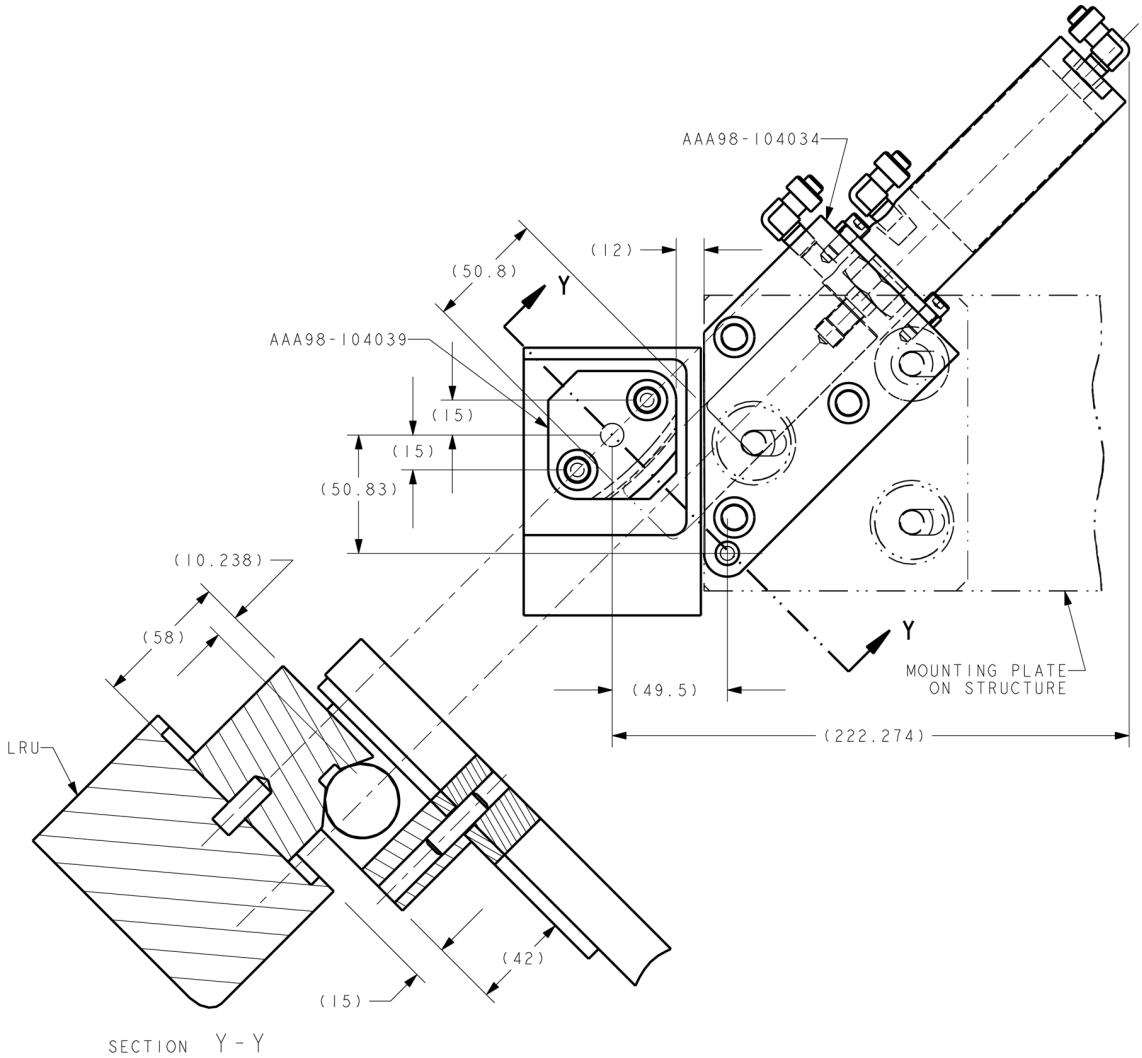

Figure 7-9 The pneumatically actuated pin extends underneath the vee block to support the LRU.

Table 7-3 shows the results of the contact analysis between the pin and vee block. These results are virtually the same as for the upper mount so the same materials, heat treatments and finishes are being used for both upper and lower mounts. The pins are made from 52100 steel to a 0.4 μm surface finish, then heat treated to 58-62 Rc, and flash chrome plated 2.5 to 5 μm in thickness. The slotted receivers and vee blocks are made from 440C stainless steel to a 0.4 μm surface finish and then heat treated to 57-60 Rc. Chrome is a hard, dissimilar material that provides greater wear resistance and lower friction. High-strength steel that has been chrome plated requires post heat treating to avoid hydrogen embrittlement. The temperature of this process is 375˚F, which is about the same as the bake-out temperature being proposed to clean small parts for NIF. Many alloy steels would lose hardness at this temperature, but 52100 steel and 440C stainless steel retain full hardness. In addition, these steels are cleaner (metallurgically speaking) than most alloy steels since their predominant use is for rolling-element bearings.

Analysis for Lower Mount		
Pin's principal radii of curvature	R_{xx} = inf. (straight)	R_{yy} = 16 mm
Vee's principal radii of curvature	R_{xx} = 150 mm	R_{yy} = inf. (straight)
Load cases: nominal and 4x nominal	P = 250 kgf	P = 4 (250) kgf
Contact pressure (compressive stress)	p = 225 ksi	p = 358 ksi
Maximum shear stress (no sliding)	τ = 71.8 ksi	τ = 114 ksi
Equivalent tensile stress $\sigma = \sqrt{3}\,\tau$	σ = 124 ksi	σ = 198 ksi
Approach of distant points	δ = 16 μm	δ = 41 μm
Stiffness at the nominal load	k = 1.29 Mlb/in	

Table 7-3 Two load cases are provided for the lower mount. Four times the nominal load represents a dynamic overload that might occur in an earthquake.

Relatively high contact stress also exists between the pin and the bore of the housing at the very edge. The close fit, 75 to 25 μm diametral clearance, picks up area rapidly around the edge so it is acceptable and perhaps preferable that the housing be relatively soft and malleable compared to the pin. Therefore, the housing is made from free-machining 303 stainless steel. A Hertz analysis is not really valid for this problem because the contact area forms an arc around the pin and the edge is not a well-defined surface. Still it is possible to obtain a rough estimate of the elastic-plastic behavior by assuming an edge radius that produces a contact pressure equal to the Brinell hardness (kgf/mm^2) of the softer material. Table 7-4 shows the results of the contact analysis using the three principal radii from the geometry and the edge radius chosen to allow yielding, R_{xx} = 8 mm. This analysis predicts a significant wrap around the pin, which is why a round bore is used rather than some other shape to act as a vee constraint. The repeatability should be more than adequate since the centering of reflective optics is not very demanding.

Analysis for Pin in Housing		
Pin's principal radii of curvature	R_{xx} = inf. (straight)	R_{yy} = 15.975 mm
Bore's principal radii of curvature	R_{xx} = 8 mm	R_{yy} = -16.0125 mm
Nominal load case	P = 410 kgf	
Contact pressure (compressive stress)	p = 233 ksi	p = 164 HBn
Arc length of contact	2 (a) = 21 mm	2 (a/r) = 74°
Width of contact	2 (b) = 0.23 mm	
Approach of distant points	δ = 9.5 μm	
Stiffness at the nominal load	k = 3.6 Mlb/in	

Table 7-4 The elastic-plastic behavior between the pin and housing of the lower mount is estimated by an elastic Hertz analysis using an edge radius that makes the contact pressure equal to the material hardness.

7.6 Tip-Tilt Mounts for NIF Large-Aperture Optics

All 192 beam lines in the NIF require up to eight large-aperture laser mirrors, LM1 through LM8, and a polarizer optic to direct light through the system. The mount for each reflective optic requires tip-tilt actuation with a program step size of the order 0.1 μr over a range of 10 mr. In addition, the mount must support the optic sufficiently well to meet the wavefront error budget and have sufficient rigidity to meet the stability budget. There are three basic mount designs being used for NIF reflective optics. One is unique to LM1 because it is a deformable mirror and not particularly challenging to mount. The second type is the topic of this section. LM2 and the polarizer require full-aperture light to pass through the mount. LM3 is very similar to the polarizer since the pair forms the periscope optics. The third type supports LM4 through LM8 from the back side where there is free access. This design features a tripod flexure with the instant center placed at the centroidal plane of the optic. The attachment points for the tripod and two actuators are chosen to minimized wavefront error. A fourth flexure constrains in-plane rotation about the tripod.

The traditional approach to a full-aperture optic mount would be a bezel that clamps the faces of the optic in one of several possible ways. Clamps at three local areas would be the most kinematic, or four clamps would be acceptable if the bezel were torsionally flexible and the clamps were initially coplanar. It is also common to use a full-length compliant element such as an o-ring. In hind sight, the bezel mount with four clamps may have posed the fewest problems, but a preconception that the optic must fit within the LRU frame left too little space for a bezel. There would have been space problems but not insurmountable ones if the bezels were external. The attractive feature of a bezel is greater freedom in how the tip-tilt mechanism fastens to the bezel rather than directly to the optic. However, with a direct mounting solution in mind, it is compelling not to use a bezel.

Figure 7-10 shows the tip-tilt mount being used for NIF periscope optics. These optics are fairly large (807 x 417 x 90 mm for the polarizer and 740 x 417 x 80 mm for LM3) and inclined 33.6˚ from a horizontal plane. A similar mount is being used for LM2 except the optic is 412 x 412 x 80 mm and in a vertical plane. There are three support points that lie in the centroidal plane of the optic. The mount provides two constraints at each point giving a total of six. As noted, two support points are actuated in the out-of-plane direction to provide tip-tilt motion. The three constraint lines and instant centers (one is off the page) help in visualizing the in-plane constraints. The physical connection between the optic and each support is a separable spherical joint. Each support must release one degree of freedom of the three defined by the spherical joint to give the required two constraints at each support. A simple flexure hinge at the passive support releases the optic along its centerline. The arm of the actuated support is free to rotate about the same bearing that provides the actuated motion. This releases motion of the optic about the upper instant center, for example. Try standing with your legs apart to simulate this motion. Your hips are equivalent to the spherical joints and your ankles are equivalent to the bearings.

The optic has three conical sockets machined into the edges to receive three plastic bearing inserts. The shape of the insert is slightly toroidal to form an annular contact with a hardened stainless steel ball. The thickness of the insert is only 0.5 mm between the conical socket and the 12 mm diameter ball. The included angle of the cone and the annular contact area is 40˚. An axial force is required to maintain engagement of the ball, insert and cone. A compression spring provides the preload for the passive support, and the weight of the optic preloads the active supports. In addition, seismic restraints prevent the supports from completely disengaging if there is not adequate preload. Several plastic materials were tested and Torlon produced the least creep and provided relatively low friction.

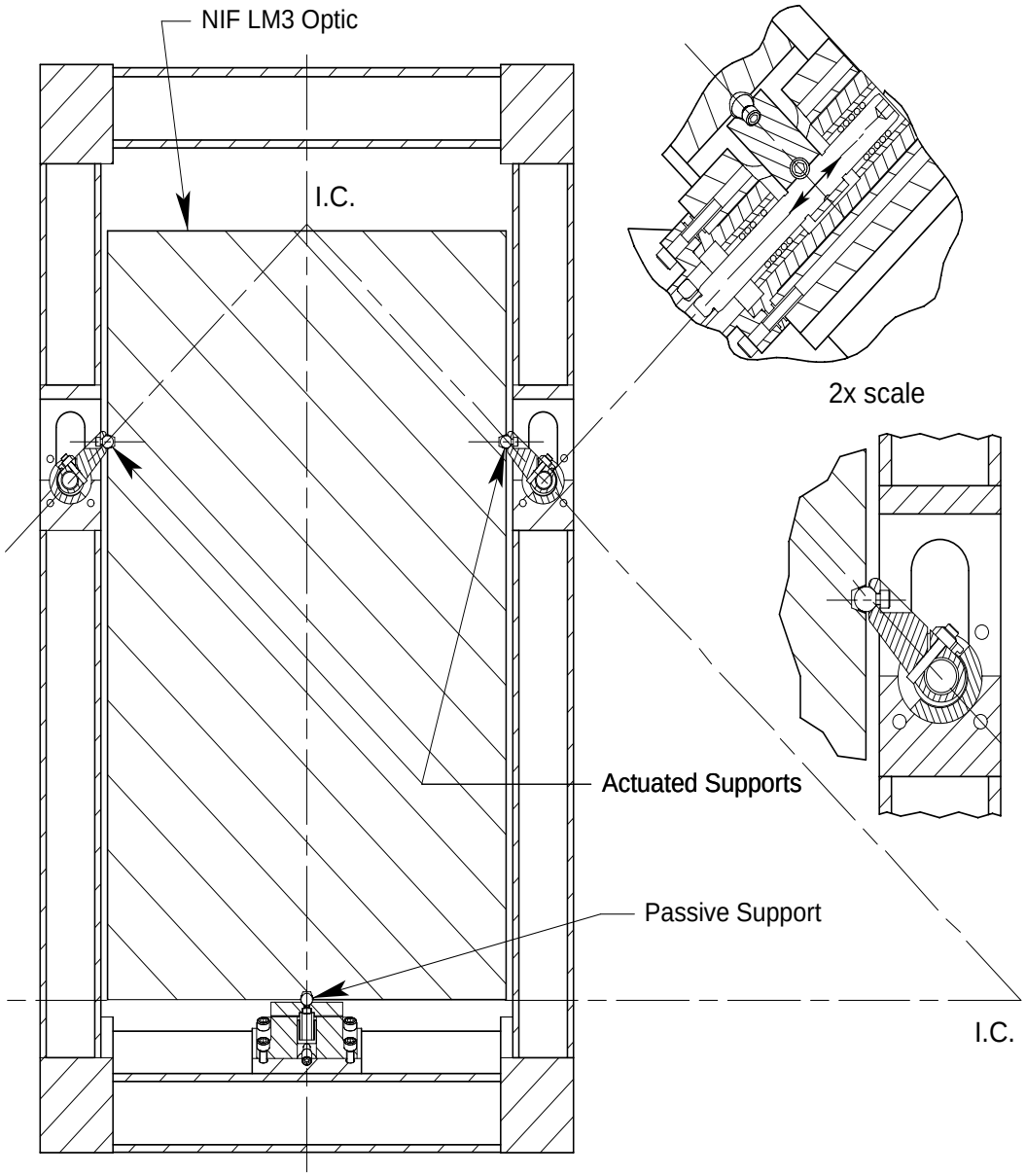

Figure 7-10 The NIF edge-style mount supports the optic at three conical sockets machined directly into the glass. Two actuated supports provide tip-tilt motion of the optic about the third passive support.